

RESEARCH

Open Access



# A novel function for $\alpha$ -synuclein as a regulator of NCK2 in olfactory bulb: implications for its role in olfaction

Jing Ren<sup>1,2†</sup>, Chao Wu<sup>1,2†</sup>, Mengxia Zeng<sup>1,2</sup>, Mingqin Qu<sup>1,2</sup>, Ge Gao<sup>1,2</sup>, Ning Chen<sup>3,4</sup>, Jingjing Yue<sup>1,2</sup>, Yuwen Jiang<sup>1,2</sup>, Tongfei Zhao<sup>1,2</sup>, Na Xiang<sup>1,2</sup>, Fangang Meng<sup>3,4</sup> and Ling-ling Lu<sup>1,2\*</sup> 

## Abstract

To investigate physiological function of  $\alpha$ -synuclein is important for understanding its pathophysiological mechanism in synucleinopathies including Parkinson's disease. Employing knockout mice, we found that Snac/ $\alpha$ -synuclein deletion induced aberrant projection of olfactory sensory neurons and hyposmia. We identified 9 axon guidance associated differentially expressed proteins using iTRAQ based Liquid Chromatograph Mass Spectrometer. NCK2 is most significantly down-regulated protein among them. We further found that either  $\alpha$ -synuclein deletion or NCK2 deficiency induced Eph A4 inactivation. Re-expressing Snac/ $\alpha$ -synuclein in its knockout neurons reversed the down-regulation of NCK2, as well as the inactivation of EphA4. Overexpression of Snac/ $\alpha$ -synuclein in  $\alpha$ -synuclein deleted mice reversed the down-regulation of NCK2 and pEphA4, and improved the olfactory impairment of mice. Correlation analysis showed that there is a significant correlation between the protein level of  $\alpha$ -synuclein, NCK2, and pEphA4, respectively. Nonetheless, immunoprecipitation analysis showed that NCK2 was associated with both EphA4 and Rho A, suggesting that NCK2 as a scaffolding protein to modulate Eph A4/Rho A pathway. Moreover, Rho A activity was significantly lower in  $\alpha$ -synuclein deficient mice. Thus,  $\alpha$ -synuclein regulates olfactory neurons projection through NCK2 dependent EphA4/Rho A pathway. Malfunction of  $\alpha$ -synuclein because of deletion may cause aberrant olfactory neurons projection. This extended our knowledge of  $\alpha$ -synuclein functions, which may explain why olfaction is usually impaired in some synucleinopathies.

**Keywords** Parkinson's disease,  $\alpha$ -synuclein, Ephs, NCK2, Synucleinopathies

## Introduction

Parkinson's disease (PD) is one of the most common neurodegenerative disorders. Its prevalence is 0.5%–1% among persons of 65–69 years old and 1%–3% among those over the age of 80 years [1]. Although the exact etiology remains unclear, it was believed that aging, genetic and environmental factors play combined roles in its pathogenesis [2, 3]. Study of genes linked to familial Parkinsonism/PD yield critical insights into mechanisms shared by sporadic and familial disease.

SNAC/ $\alpha$ -synuclein ( $\alpha$ -syn) is the first genetic mutation identified in a Italian heritable PD family. It is responsible for an autosomal-dominant form

<sup>†</sup>Jing Ren and Chao Wu contributed equally to this work.

\*Correspondence:

Ling-ling Lu  
lllu@ccmu.edu.cn

<sup>1</sup> Department of Neurobiology, Capital Medical University, 10 You'an Men Wai, Xitoutiao, Beijing 100069, China

<sup>2</sup> Key Laboratory for Neurodegenerative Diseases of the Ministry of Education, Beijing 100069, China

<sup>3</sup> Department of Functional Neurosurgery, Beijing Tiantan Hospital, Capital Medical University, Beijing 100070, China

<sup>4</sup> Department of Functional Neurosurgery, Beijing Neurosurgical Institute, Capital Medical University, Beijing 100070, China



of PD.  $\alpha$ -syn is a small, well-conserved protein that is expressed in many tissues and cell types [4–6]; its main protein domains comprise an amphipathic region, non-amyloid- $\beta$  component (NAC) domain and an acidic tail [7–9]. Single point mutations in SNAC/ $\alpha$ -syn will lead to early onset PD [10–15]. Moreover, triplication of the gene locus [16, 17] and its polymorphisms are also associated with high risk of PD [18, 19].  $\alpha$ -syn is not only associated with familial Parkinsonism, it also has been shown to have a central pathogenic role in sporadic PD [20, 21]. Accumulated  $\alpha$ -syn is reported to be the main component of Lewy bodies (LBs), the hallmark of PD. Hence,  $\alpha$ -syn is the most potent culprit underlying PD. However, both pathogenic mechanisms underlying  $\alpha$ -syn with PD and its physiological function remains unclear.

As a neurodegenerative movement disorder, PD is commonly characterized by motor symptoms such as resting tremor, rigidity, akinesia, bradykinesia, and postural instability [22, 23], due to the loss of Nigral dopaminergic neurons and a decrease in the dopamine (DA) contents of the caudate-putamen structures [24]. However, the onset of PD is considered to commence at least 20 years prior to detectable motor deficits. This period is referred to as the prodromal stage when a variety of non-motor symptoms such as olfactory dysfunction, sleep disturbances, obesity and depression etc. can be observed. Olfactory dysfunction is one of the prodromal symptoms and precede motor abnormalities by 20 years [25, 26]. The reported prevalence of olfactory impairment in PD range from 45 to 90%. Nonetheless, Braak and colleagues reported that  $\alpha$ -syn pathology was observed in olfactory bulb (OB) in very early stage of PD. In his theory, OB, as one of sensory organs opening to the outside, is susceptible to toxic environment and easy to deteriorate. An external stimuli such as pesticide rotenone and herbicide Paraquat are transmitted through the nasal mucosa to the OB, causing  $\alpha$ -syn pathology within the OB [27, 28]. Hence, OB is one of the original sites of  $\alpha$ -syn pathology. Then study the physiological function of  $\alpha$ -syn in olfactory system will be helpful to understand the onset and progress of PD.

Here, we use Snac/ $\alpha$ -syn knockout (Snac<sup>-/-</sup>, KO) mice and its wild-type (Snac<sup>+/+</sup>, WT) littermate as a control to study the influence of  $\alpha$ -syn deficiency on mice olfaction. The Snac<sup>-/-</sup> mice exhibited aberrant projection of olfactory sensory neurons (OSNs) and olfactory dysfunction accordingly. NCK2, identified by proteomics sequencing, and its downstream Eph A4/Rho A were shown to be associated with this  $\alpha$ -syn efficiency-induced aberrant projection.

## Materials and methods

### Animals

All the animal experiments were conducted in accordance with the National Institutes of Health guidelines on the care and use of laboratory animals, and were approved by the Animal Care Committee of Capital Medical University. We used male Snac KO mice and their male wild-type (WT) littermates for the present study. Snac KO and WT mice were group housed in a room with a 12 h light/dark cycle (lights on at 7:00 a.m.), with access to food and water ad libitum. Room temperature was kept at 23 ± 2 °C. For  $\alpha$ -syn rescue experiments, adeno-associated virus carried Snca (AAV-Snac) was injected into olfactory bulb of Snac KO mice. KO mice injected with AAV without Snac were used as negative control. Olfaction behavior test were done 6 months later.

### Western blot

Equal amounts of protein (100  $\mu$ g) were separated by 10% sodium dodecyl sulfate polyacrylamide gel electrophoresis and then transferred to a PVDF membrane (Pall Co., Taiwan) that was blocked in 5% non-fat milk for 1 h at room temperature and incubated overnight with primary antibodies against the following proteins:  $\alpha$ -synuclein (1:1000, BD, NJ, USA), NCK2 (1:1000, Sigma-Aldrich, MO, USA), pEphA1 (1:500, Abcam, Cambridge, UK), pEphA2 (1:500, Abcam, Cambridge, UK), pEphA3 (1:500, Abcam, Cambridge, UK), pEphA4 (1:500, Abcam, Cambridge, UK), pEphA5 (1:500, Abcam, Cambridge, UK), pEph B1/B2 (1:500, Abcam, Cambridge, UK) and  $\beta$ -actin (1:1000, Sigma-Aldrich, MO, USA). Immuno-reactivity was detected with Fluorescence-conjugated anti-mouse or -rabbit antibodies (1:10,000; Sigma-Aldrich, MO, USA).

### Immunohistochemistry

Mice were sacrificed and brains were fixed with 4% paraformaldehyde and sectioned at a 50- $\mu$ m thickness. The staining was carried out on free-floating sections. Sections were rinsed in PBS and incubated in 3% H<sub>2</sub>O<sub>2</sub> for 20 min to block the endogenous peroxidase activity. After washing in PBS, sections were incubated in blocking serum (10% goat serum and 0.1% Triton X-100 in PBS) for 30 min, followed by incubation in anti- $\alpha$ -synuclein antibody solution (1:1000, BD, NJ, USA) or olfr1507 (1:1000, Thermo Fisher, MA, USA) for 24 h at 4 °C. Then, the sections were incubated with Alexa 594-conjugated goat anti-mouse IgG (1:1000, Cell Signaling Technology, MA, USA) for 2 h at room temperature. Images were captured by a Leica confocal microscope (Leica Microsystems, Wetzlar, Germany).

### Quantitative real time PCR

Total RNA was isolated from the OB of  $\alpha$ -syn/Snac KO or its WT littermate control using the RNeasy Mini kit (Qiagen, Düsseldorf, Germany). 5  $\mu$ g RNA were reverse-transcribed in a reaction containing 1  $\mu$ l dNTP (10 mmol/l; Invitrogen), 0.5  $\mu$ g oligo (dT) primer, with 50 U Superscript RNase reverse transcriptase (Invitrogen, CA, USA) for 50 min at 42 °C. Forward and reverse primer sequences for PCR were as follows:  $\beta$ -actin, 5'-ACC ACC ATG TAC CCA GGC ATT-3' and 5'-CCA CAC AGA GTA CTT GCG CTC A-3'; *NCK2*, 5'-GTC ATAGCCAAGTGGGACTACA-3' and 5'-GCACGT AGCCTGTCCTGTT-3'. The reaction was carried out on 7500 real-time PCR systems (Applied Biosystems, Foster City, CA, USA) using the default thermal cycling conditions (2 min at 50 °C plus 10 min at 95 °C for the hot start; and 40 cycles of 15 s at 95 °C plus 1 min at 60 °C).

### iTRAQ based liquid chromatograph mass spectrometer (LC-MS)

OB tissue were taken from 8-week-old male  $\alpha$ -syn/Snac KO mice and their male wild-type littermates. Two biological replicates of each group were prepared for the proteomics experiments. Briefly, the total protein of OB was grinded and dissolved in lysis buffer [9 M Urea, 4% CHAPS, 1% DTT, 1% IPG buffer (GE Healthcare, IL, USA)]. The mix was incubated at 30 °C for 1 h and centrifuged at 15,000g for 15 min at room temperature. The supernatant was collected and quantified by the Bradford method.

100  $\mu$ g of protein of each sample was dissolved in a dissolution buffer (AB Sciex, Foster City, CA, USA). After being reduced, alkylated and trypsin-digested, the samples were labeled following the manufacturer's instructions for the iTRAQ Reagents 8-plex kit (AB Sciex, Foster City, CA, USA). Samples were each labeled with iTRAQ reagents with molecular masses of 113, 114, 115, and 116 Da, respectively. After labeling, all samples were pooled and purified using a strong cation exchange chromatography (SCX) column by Agilent 1200 HPLC (Agilent, CA, USA) and separated by liquid chromatography (LC) using a Eksigent nanoLC-Ultra 2D system (AB SCIEX, CA, USA). The LC fractions were analyzed using a Triple TOF 5600 mass spectrometer (AB SCIEX, CA, USA). Mass spectrometer data acquisition was performed with a Triple TOF 5600 System (AB SCIEX, CA, USA) fitted with a Nanospray III source (AB SCIEX, CA, USA) and a pulled quartz tip as the emitter. Data were acquired using an ion spray voltage of 2.5 kV, curtain gas of 30 PSI, nebulizer gas of 5 PSI, and an interface heater temperature of 150 °C. For information dependent acquisition (IDA), survey scans

were acquired in 250 ms and as many as 35 product ion scans were collected if they exceeded a threshold of 150 counts per second (counts/s) with a 2<sup>+</sup> to 5<sup>+</sup> charge-state. The total cycle time was fixed to 2.5 s. A rolling collision energy setting was applied to all precursor ions for collision-induced dissociation (CID). Dynamic exclusion was set for 1/2 of peak width (18 s), and the precursor was then refreshed off the exclusion list.

The iTRAQ data were processed with Protein Pilot Software v4.0 against the *A. japonicus* database using the Paragon algorithm. Protein identification was performed with the search option of emphasis on biological modifications. The database search parameters were the following: the instrument was Triple TOF 5600, iTRAQ quantification, cysteine modified with iodoacetamide; biological modifications were selected as ID focus, trypsin digestion. For false discovery rate (FDR) calculation, an automatic decoy database search strategy was employed to estimate FDR using the PSPEP (Proteomics System Performance Evaluation Pipeline Software, integrated in the ProteinPilot Software). The FDR was calculated as the number of false positive matches divided by the number of total matches. Then, the iTRAQ was chosen for protein quantification with unique peptides during the search, and peptides with global FDR values from fit less than 1% were considered for further analysis. Within each iTRAQ run, differentially expressed proteins were determined based on the ratios of differently labeled proteins and p-values provided by Protein Pilot; the p-values were generated by Protein Pilot using the peptides used to quantitate the respective protein. Finally, for differential expression analysis, fold change was calculated as the average ratio of 113/114, 113/116, 115/114 and 115/116. Proteins with a fold change of >1.5 or <0.67 and p < 0.05 were considered to be significantly differentially expressed.

### Rho A activation assay

Assays for the active form of Rho A was performed, as described previously [45]. Briefly, primary neurons were seeded on 24 mm dishes and cells were cultured to approximately 85–90% confluence. Cells were lysed in Mg<sup>2+</sup> + Lysis/Wash Buffer containing 25 mM HEPES, pH 7.5, 150 mM NaCl, 1% Igepal CA-630, 10 mM MgCl<sub>2</sub>, 1 mM EDTA and 2% glycerol, supplemented with 10  $\mu$ g/mL aprotinin and 10  $\mu$ g/mL leupeptin and subjected to Rho A pull-down assays with rhotekin RBD agarose (Millipore, MA, USA), which would bind and detect active RhoA. GTP bound RhoA was separated on SDS-polyacrylamide gel electrophoresis gels and subjected to Western blot analysis with the RhoA antibody.

### Quantification and statistical analysis

Data are expressed as mean  $\pm$  SD. The sample size ( $n$ ) represents biological replicates. Student's  $t$  test was used for comparison of two group averages. When there were more than two groups, one-way ANOVA Tukey–Kramer multiple comparisons Bonferroni post hoc test was performed. All the bioinformatics were analyzed or confirmed by bioinformaticians. iTRAQ based LC–MS analysis was performed in a double-blinded manner. A  $P$  value  $< 0.05$  was considered statistically significant.

## Results

### $\alpha$ -syn was abundantly expressed in both olfactory epithelium and OB

In order to investigate  $\alpha$ -syn expression pattern in the brain, western blot was used to evaluate  $\alpha$ -syn protein level in different brain regions eg. cortex (Crt), cerebellum (Cere), OB, olfactory epithelium (OE), striatum (Str) and substantia nigra (SN). As was shown in Fig. 1,  $\alpha$ -syn was abundant in olfactory system, especially in OB. Immunofluorescence staining showed that  $\alpha$ -syn is specifically expressed in the soma of olfactory sensory neurons (OSNs) and the olfactory bundles of OE.  $\alpha$ -syn was also observed in olfactory glomeruli and outer plexiform layer of OB (Fig. 1).

### $\alpha$ -syn deficiency induced aberrant projection of OSNs and resulted in hyposmia

As we know, the mapping of OSNs onto glomeruli astonishingly precise. Each glomerulus receives axons from a large number of OSNs that express the same olfactory receptor (OR). So doing immunofluorescence staining of OB with one specific OR antibody, only one positive glomerulus in each bulb will be detected. Olfr1507, one kind of OR, antibody was used to evaluate the axon projection in  $\alpha$ -syn/Snac KO mice in the present study. Of note, Olfr1507 positive axons projected aberrantly in  $\alpha$ -syn deficient mice. Some Olfr1507 positive axons projected to external plexiform layer. Some projected to the inner plexiform layer. And some projected out of the glomerulus although it still locates in the glomerulus layer (Fig. 2). Buried pellet test and two-bottle preference test were used to evaluate the olfactory function of  $\alpha$ -syn deficient (KO) mice. In the buried food test, KO mice spent more time to locate the buried pellet compared with WT mice by 6 months ( $P < 0.01$ , Fig. 2). In the two-bottle preference test, there were no significant differences between the strains in water intake before 3 months age. The littermate KO mice started to consume water from bottle treated with 0.7% hydrochloride acid at 6 months old and kept increasing at 9 months old, however, control animals

still displayed a strong preference for water from non-treated bottle. ( $P < 0.05$  for 6 months and  $P < 0.01$  for 9 months, Fig. 2).

### 9 axon guidance associated proteins was identified by iTRAQ based LC–MS

In KO mice, Olfr1507 positive axons project aberrantly which indicates that  $\alpha$ -syn played an important role in olfactory axons guidance. To find out the molecules involved in this process, iTRAQ based LC–MS was carried out to compare the differentially expressed proteins between KO mice and its litter mate control.

The screening criteria of reliable proteins: Unique peptide  $\geq 1$ , remove invalid values and the anti-library data, and screening significant differentially expressed protein based on the reliable proteins. The screening criteria of differentially expressed protein: Fold change is 1.5. Changes greater than 1.5 or less than 0.67 are considered to be differentially expressed proteins. Screening results statistics of differentially expressed proteins were as follows:

1. Total number of all proteins: 5489 pcs.
2. Total number of reliable proteins: 4936 pcs.
3. Number of differentially expressed proteins in Dynamics: 278 pcs.
4. The number of differentially expressed proteins in Snac KO mice and its litter mate control: 188 pcs.

Among all above 188 differentially expressed proteins, 133 were up-regulated and 55 were down-regulated (Fig. 3). Further analysis showed that 9 of differentially expressed proteins were associated with axon guidance (Table 1). The expression level of these 9 differentially expressed proteins was first verified by quantitative real-time RT-PCR. The results showed that 5 of them including Cdh4, Cldn5, Dscam, Eif2b2, Pllp, Snapin were up-regulated and 4 of them including Snapin, Spag1, Stk11 and NCK2 were down-regulated. NCK2 was one of the most significant one that down-regulated by  $\alpha$ -syn deletion.

### $\alpha$ -syn modulated NCK2 protein expression level

Cytoplasmic protein NCK2, one of the most significant down-regulated proteins, is shown to bind and recruit various proteins involved in the regulation of receptor tyrosine kinases family (RTKs). Bioinformatic analysis for NCK2 showed that it takes part in the following biological process, eg. actin filament organization, cell migration, Ephrin receptor signaling pathway, positive regulation of actin filament polymerization, signal complex assembly and signal transduction. The first 4 process are directly associated with axon guidance and

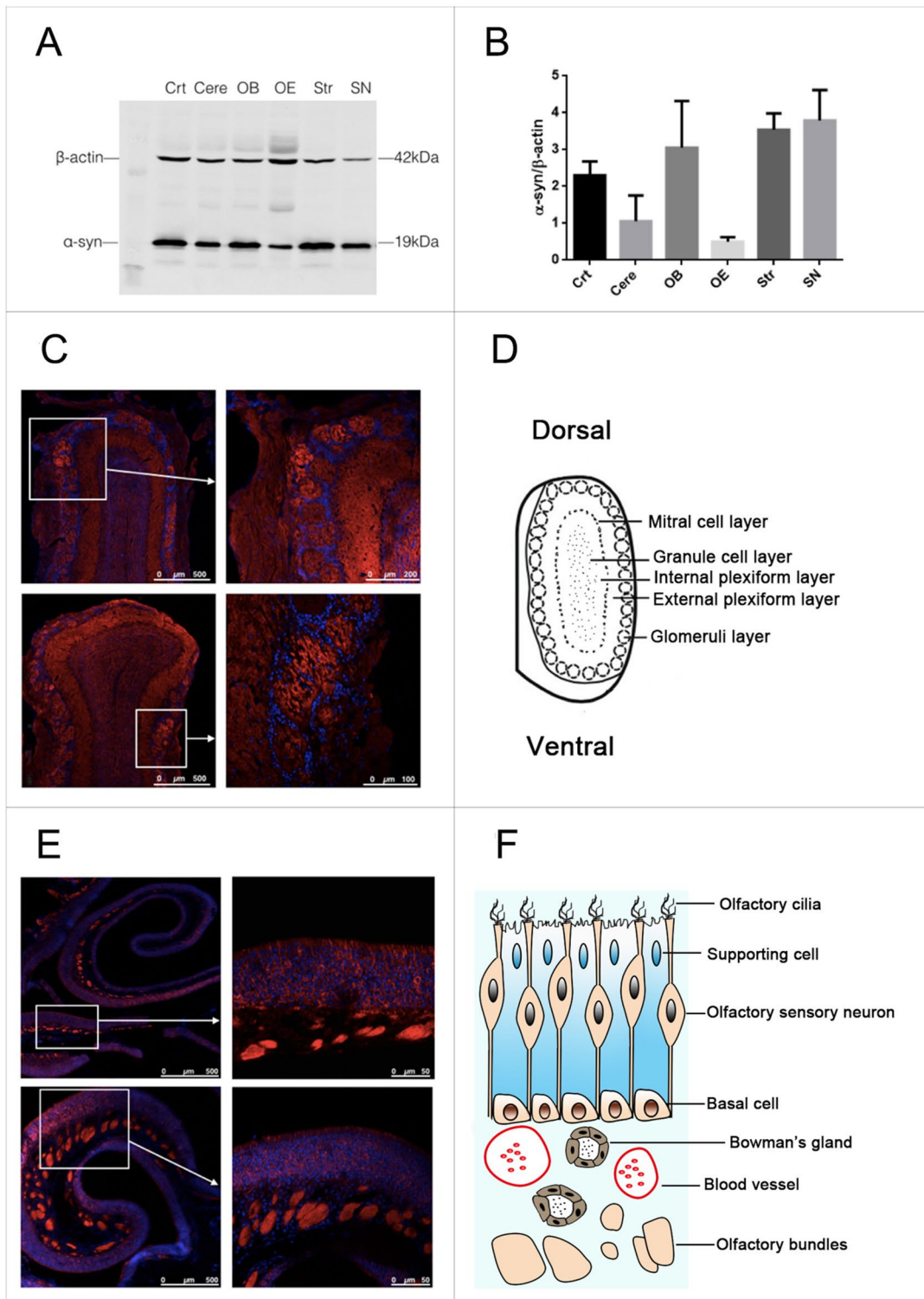


**Fig. 1** α-syn was abundant in both olfactory epithelium and OB. **A, B** α-syn was expressed in different brain regions. α-syn protein level was investigated in various brain regions. It was abundant in olfactory system, especially in OB. Data are expressed as mean ± SD, N=3. **C** Immunofluorescence staining to show α-syn expression pattern in OB. α-syn was mainly located on olfactory glomeruli and outer plexiform layer of OB. **D** Schematic diagram of OB. **E** Immunofluorescence staining to show α-syn expression pattern in OE. α-syn is abundant in the soma of OSNs and olfactory bundles of OE. **F** Schematic diagram of OE

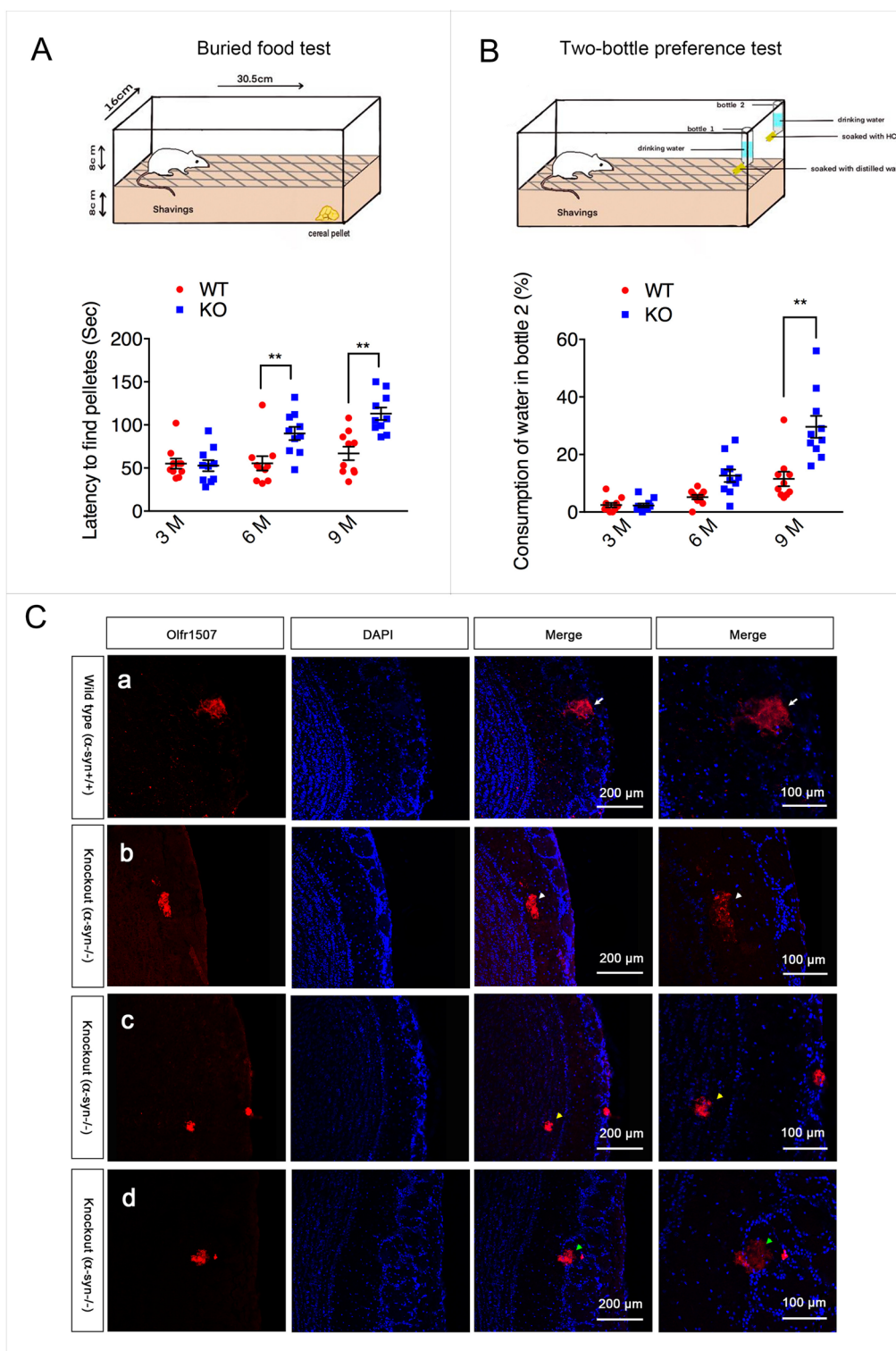


**Fig. 2**  $\alpha$ -syn deficiency induced olfaction impairment and aberrant projection of olfactory neurons. **A** Statistical results of buried food pellet test. Data are expressed as the mean  $\pm$  SEM. **B** Statistical results of two-bottle preference test. Data are expressed as the mean  $\pm$  SEM. **C** Immunofluorescence staining using an antibody against the Olf1507 revealed that Olf1507-expressing OSNs axon fibers converge to one specific glomerulus in each half bulb in wild type mice (WT,  $\alpha$ -Syn<sup>+/+</sup>) as indicated by the white arrow. In  $\alpha$ -Syn null mice (KO,  $\alpha$ -Syn<sup>-/-</sup>), Olf1507-expressing OSNs axons projected aberrantly. Some Olf1507 positive axons projected to external plexiform layer as indicated by the white arrowhead. Some projected to the inner plexiform layer as indicated by the yellow arrowhead. And some projected out of the glomerulus although it still locates in the glomerulus layer as indicated by the green arrowhead

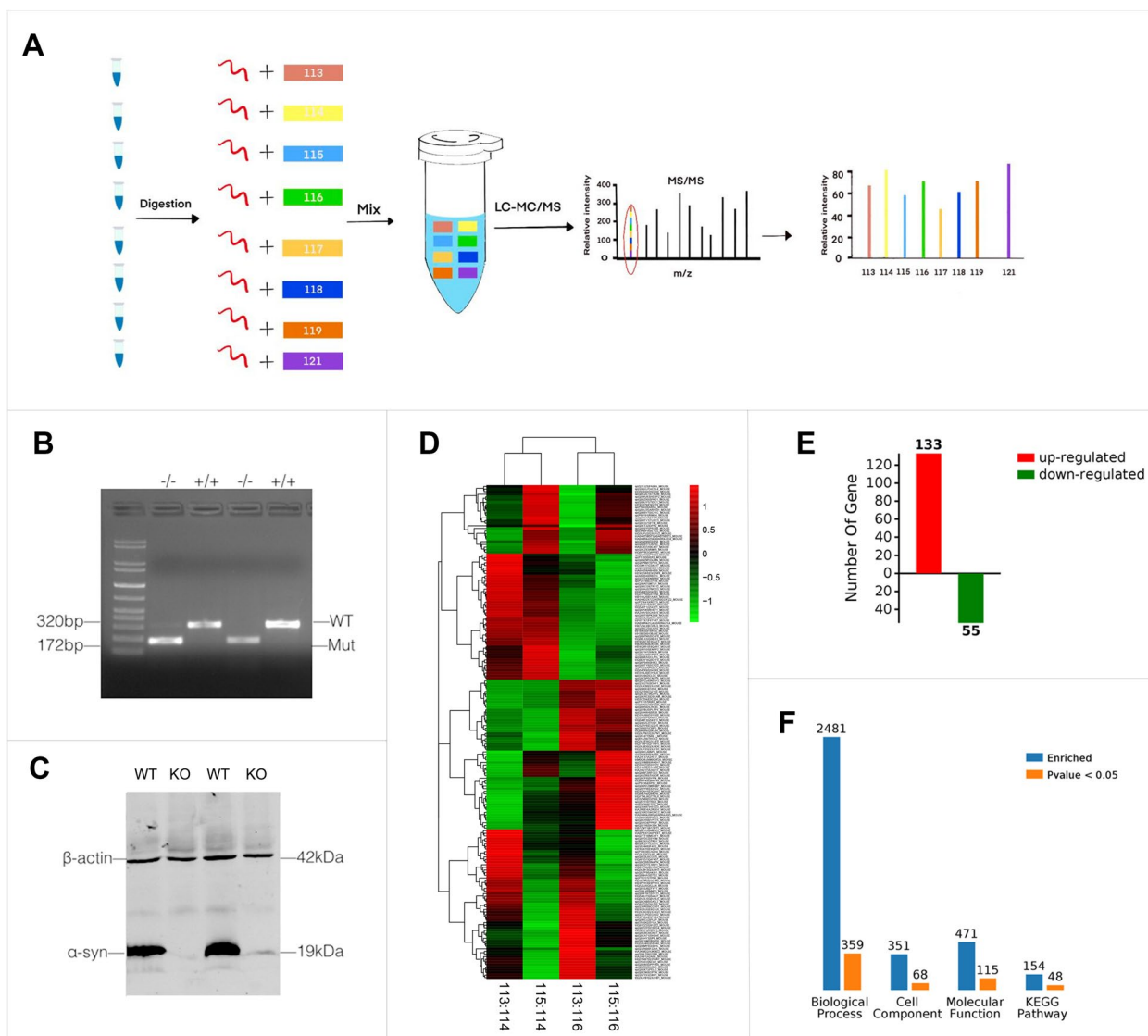


**Fig. 3** Identification of differentially expressed proteins in  $\alpha$ -syn null mice by iTRAQ based LC-MS. **A** Flow chart for differentially expressed proteins identification. **B, C** Genotyping and western blotting to confirm the mice genotype. **D** The heatmap for the differentially expressed proteins. In the heatmap, red color represents up-regulated differentially expressed proteins and the green color represents down-regulated differentially expressed proteins. **E** statistical summary for differentially expressed proteins. A total of 188 proteins, can be seen in the figure in the difference comparison group. There are 133 pcs of up-regulation (red) of the protein and 55 pcs of down-regulation (green) of the protein. **F** All the differences in protein GO enrichment (BP, CC, MF) and pathway KEGG enrichment results and significant ( $p < 0.05$ ) number were summarized. The blue column represents the total number of enrichment, orange column represents a significant number of enrichment. A protein is usually involved in a number of functions or pathways, so the total number of GO enrichment and pathway KEGG enrichment results will be far greater than the number of differentially expressed proteins. The significant function or the pathway means that the difference of the enrichment to the function or the pathway is significant

the last two process are also related to the axon guidance indirectly. The following molecular function analysis showed that it exhibited cytoskeletal anchor activity, receptor tyrosine kinase binding function, signal adaptor and signaling receptor complex adaptor activity. All the above molecular functions implicated that it takes part in axonal guiding. Cellular component analysis indicated

its subcellular localization of post-synapsis are consisting with its function-axon guidance (Fig. 4A).

As shown above, NCK2 is also one of the most significantly down-regulated proteins in  $\alpha$ -syn/Snac KO mice in the present study (Table 1). So we chose NCK2 as the following research focus. The down-regulation of NCK2 was further confirmed both in mRNA level and

**Table 1** Axon guidance associated differentially expressed proteins

NO	Protein	Full name	Ratio
1	Cdh4	Cadherin-4	1.66
2	Cldn5	Claudin-5	2.21
3	Dscam	Down syndrome cell adhesion molecule homolog	1.86
4	Eif2b2	Translation initiation factor eIF-2B subunit beta	1.51
5	Plip	Plasmolipin	1.57
6	Snapi	SNARE-associated protein Snapin	0.64
7	Spag1	Sperm-associated antigen 1	0.66
8	Stk11	Serine/threonine-protein kinase	0.52
9	NCK2	Cytoplasmic protein NCK2	0.58

protein level by real-time RT-PCR and western-blotting (Fig. 4B, C). Nonetheless, the NCK2 down-regulation was reversed by overexpression of  $\alpha$ -syn in the SNAC<sup>-/-</sup> primary cultured neurons (Fig. 4D). On the other side,  $\alpha$ -syn overexpression also induced NCK2 up-regulation in protein level (Fig. 4E).

#### NCK2-EphA4 was involved in the mis-guidance of olfactory sensory neurons

Bioinformatics analysis showed that 20 proteins eg. EphA1, EphA2, EphA4, Eph A5, EphB1, EphB2, EphB3, EphB4, EfnB1, EfnB2, Eplg7, Pik3cb, NCK1, wasl, cdc42, pak3, Arhgef7, Nphs1, pak2, pard6a, were enriched in Protein-Protein Interaction (PPI) network with NCK2 ( $p < 1.0e-16$ ) (Fig. 5A). Analysis for the Network Analysis PPI between NCK2 and Ephs family showed that NCK2 associated with all of the Ephs family members. Most of them were known interactions experimentally determined (Fig. 5B). Kyoto Encyclopedia of Genes and Genomes (KEGG) analysis for these 20 proteins suggested that 16 were enriched in axon guidance pathway (Fig. 5F). Biological process (BP) analysis showed that 11 of them were enriched in Ephrin receptor signaling pathway, one of the important axon guidance pathways. 16 out of 20 proteins were involved in movement of cell or subcellular component. 14 were involved in cell migration and 14 were involved in localization of cell. All these biological process are associated with axon guidance directly or indirectly (Fig. 5C). Molecular function (MF) analysis showed that 8 out of 20 proteins exhibited Ephrin receptor activity. And some of the proteins take part in trans-membrane Ephrin receptor activity, trans-membrane receptor protein tyrosine kinase activity, phospho-transferase activity, kinase activity which are associated with axon guidance directly or indirectly (Fig. 5D). Cellular component (CC) analysis showed

that most of the proteins were located on membrane which are also consistent with their axon guiding function (Fig. 5E). Taken together, both gene ontology (GO) including BP, MF and CC analysis, and KEGG analysis implicated that NCK2 participated axon guidance via Ephrin receptor signaling pathway.

Ephrin receptor signaling pathway, also known as Eph/Ephrin signaling pathway consists of Eph receptors and Ephrin ligands. The Ephs are the largest family of RTKs in vertebrates, and are composed by A- and B-subfamilies. As mentioned above, NCK2 is able to bind and recruit various proteins involved in the regulation of RTKs. And one of the important process that NCK2 participated included ephrin receptor signaling pathway. Nonetheless, NCK2, an adaptor protein consists of one SH2 domain and 3 SH3 domains, can also binds to the tyrosine residues of RTKs via its SH2 domain (Fig. 6A). The axon guidance pathway showed that both Eph A and Eph B receptor signaling pathway involved in axon guidance, either on repulsion or attraction (Fig. 7).

Hence, to find out whether Ephrin receptor signaling pathway involved in the aberrant axon projection of olfactory sensory neurons induced by  $\alpha$ -syn deficiency, all 9 Eph receptors in the above NCK2 network were examined in Snac<sup>-/-</sup> mice. As shown in Fig. 6B, C, among 9 of Ephs, EphA4 was inactivated which was indicated by its lower phosphorylated level in  $\alpha$ -syn deficient mice. While the other 8 Ephs didn't change with  $\alpha$ -syn deficiency. Moreover, knocking-down NCK2 led to EphA4 inactivation as well (Fig. 6D-F).

To further confirm that NCK2-EphA4 was modulated by  $\alpha$ -syn, the primary cultured  $\alpha$ -syn<sup>-/-</sup> neurons were transfected with LV- $\alpha$ -syn. NCK2-EphA4 pathway was evaluated by western blot. As shown above, NCK2 and phosphorylated EphA4 were down-regulated in  $\alpha$ -syn<sup>-/-</sup> neurons, (Fig. 6G-I) indicating that NCK2-EphA4 pathway was deactivated. However, the down-regulation of NCK2 and phosphorylated EphA4 were reversed by overexpression of  $\alpha$ -syn.

#### Overexpression of $\alpha$ -syn reversed the down-regulation of NCK2 and pEphA4, and improved hyposmia of $\alpha$ -syn deficient mice

We confirmed that  $\alpha$ -syn and NCK2 played important roles in modulating Eph A4 activity by knocking-down or overexpressing of these two genes in the above experiments. As is shown above,  $\alpha$ -syn and NCK2 were involved in the olfaction impairment in  $\alpha$ -syn/Snac KO mice. We further overexpressed  $\alpha$ -syn in 4-week-old KO mice to observe whether it could improve the symptoms of olfactory dysfunction in mice (Fig. 8A, B). The results showed that overexpression of  $\alpha$ -syn could alleviate olfactory dysfunction in mice. Moreover, the down-regulation

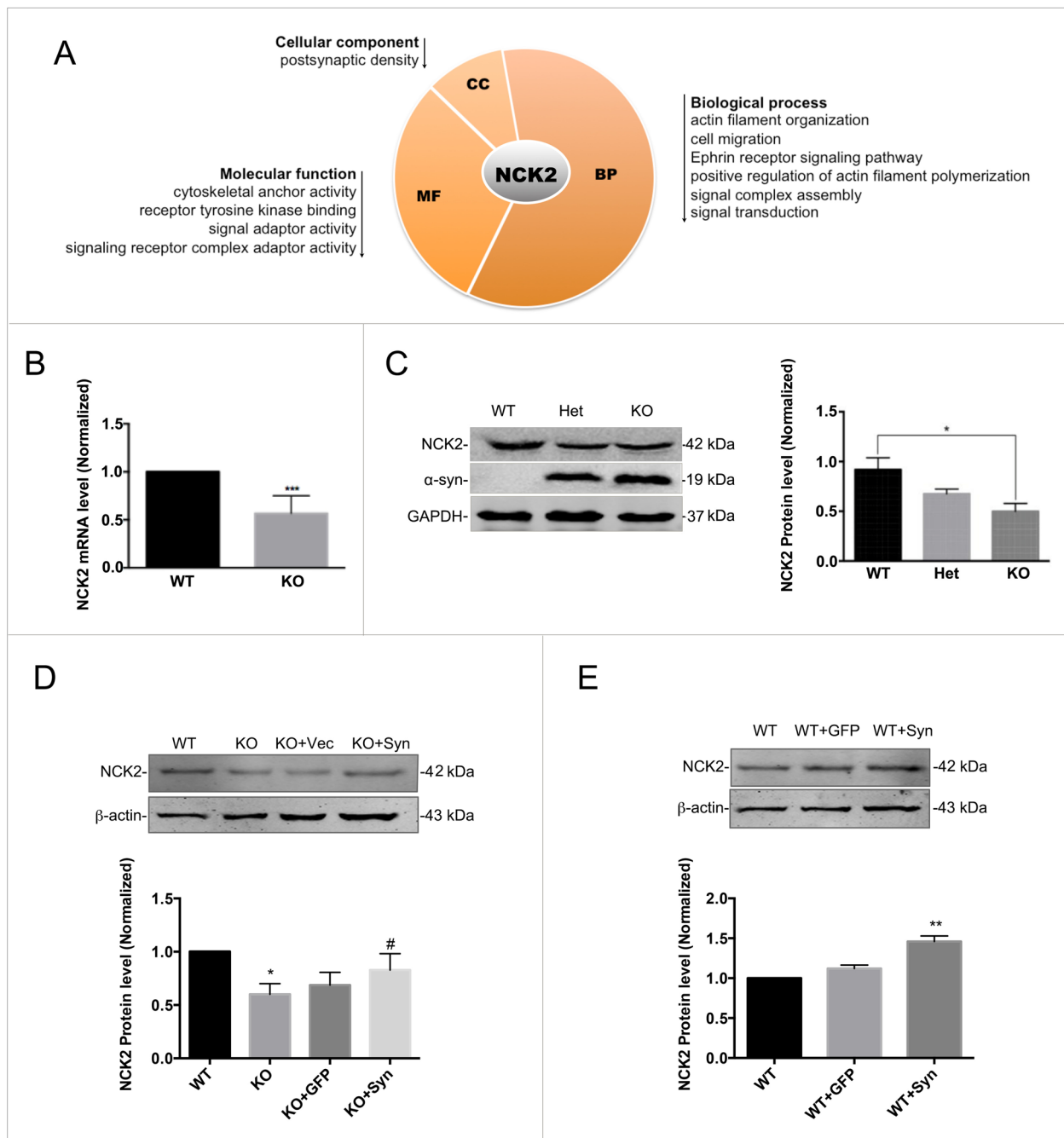


**Fig. 4** α-syn regulated the protein expression level of NCK2. **A** Bioinformatics analysis for the most down-regulated protein, NCK2 showed that NCK2 was mainly located in the postsynaptic density. Its function involved in cytoskeletal anchor, signal adaptor, cell migration etc. **B** NCK2 down-regulation was further confirmed in mRNA level by real-time RT-PCR. Data are expressed as mean ± SD. \*\*\*p < 0.001 compared to WT. **C** NCK2 down-regulation was further confirmed in protein level by western-blot. Data are expressed as mean ± SD. \*p < 0.05 compared to WT. **D** α-syn rescue experiment. NCK2 down-regulation was reversed by overexpression of α-syn in the α-syn<sup>-/-</sup> primary cultured neurons. Data are expressed as mean ± SD. \*p < 0.05, compared to WT; #p < 0.05 compared to KO; n = 3. **E** α-syn overexpression also induced NCK2 up-regulation. Data are expressed as mean ± SD. \*\*p < 0.01 compared to WT; n = 3

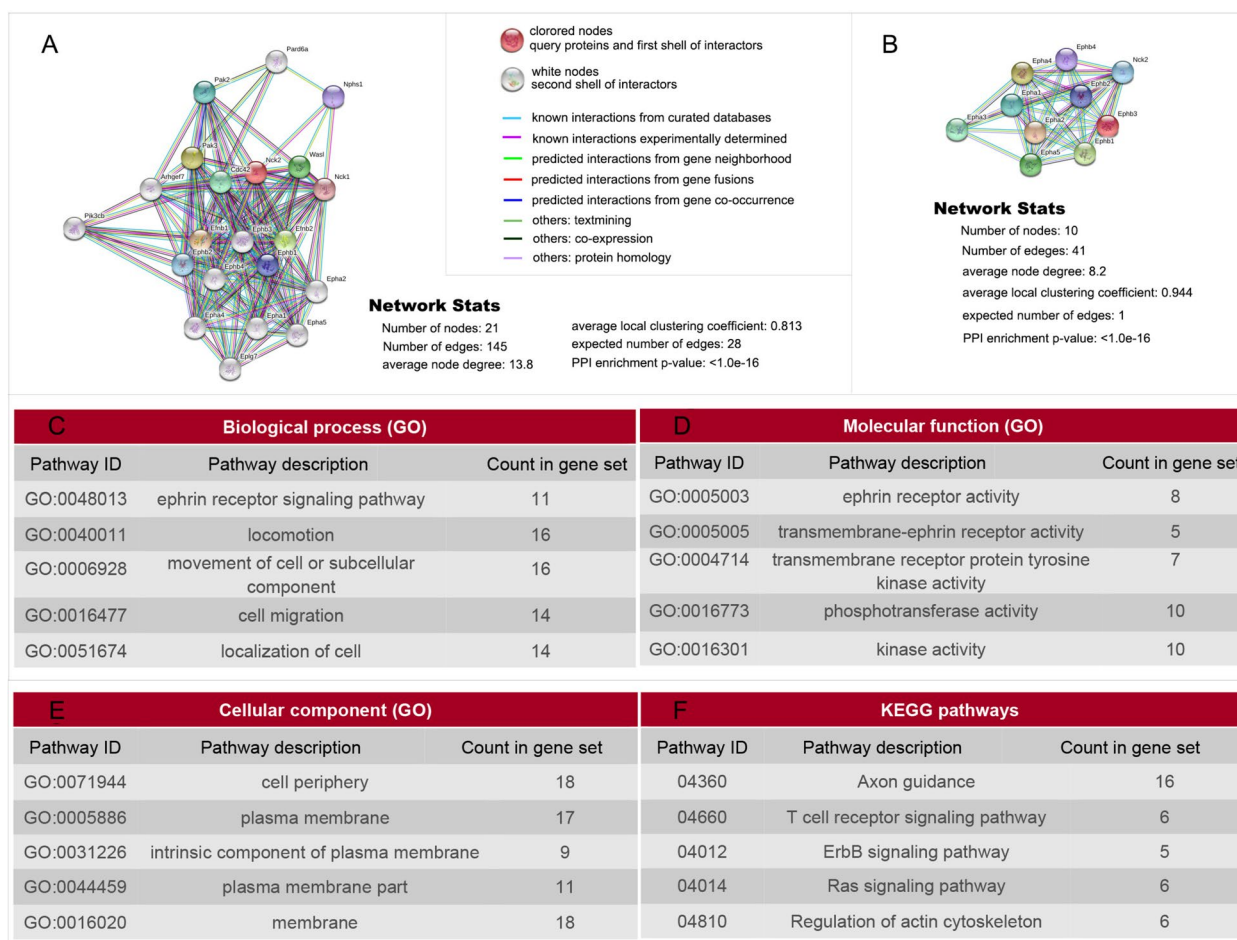


**Fig. 5** Bioinformatics analysis showed that 21 proteins were enriched in PPI network with NCK2. **A** PPI network with NCK2. Bioinformatics analysis showed that 21 proteins were enriched in PPI network with NCK2. Biological analysis for these 21 proteins showed that 11 of them were enriched in Ephrin receptor signaling pathway. **B** Further analysis on the association of NCK2 and all Ephrin receptors. And indirect or predicted interactions existed in NCK2 and Eph A1-A5, EphB1-B4. **C** GO analysis showed that all these 21 proteins involves the following biological process: Ephrin receptor signaling pathway, locomotion, movement of cell or subcellular component, cell migration, localization of cell. **D** GO analysis showed that all these 21 proteins involves the following molecular function: Ephrin receptor activity, trans-membrane receptor protein tyrosine kinase activity etc. **E** GO analysis showed that all these 21 proteins were localized on cell periphery, plasma membrane. **F** KEGG analysis showed that all these proteins involves axon guidance etc.

of NCK2 and pEphA4 were also reversed (Fig. 8C). We then analyzed the correlation among  $\alpha$ -syn, NCK2 and pEphA4. As was shown in Fig. 8D, E, there is a significant correlation between  $\alpha$ -syn, NCK2, and pEphA4, respectively,

**NCK2 was associated with EphA4 and NCK2 down-regulation led to lower Rho A activity**

As shown above (Fig. 6A), it was reported that NCK2, as an adaptor protein, binds to the phosphorylated tyrosine residue of the upstream signal protein eg. RTKs via SH2 domain and binds to the proline rich domain of the downstream signal protein eg. Rho A via SH3 domain. Ephs family and Rho A signaling pathway plays

important roles in axon guidance. Hence, to address the molecular mechanism how NCK2 involved in the misguidance of OSNs induced by  $\alpha$ -syn deficiency, we investigate the association among NCK2, Eph A4 and Rho A using immunoprecipitation assay. The results showed that NCK2 could preferentially interact with Rho A and Eph A4 (Fig. 9A). Nonetheless, less Eph A4 and Rho A were pulled-down when immunoprecipitated by using NCK2 antibody in KO mice than WT mice (Fig. 9B).

To investigate the downstream signal protein Rho A activity, RBD pull-down assay was employed to determine the active Rho A levels in primary neurons of Snac / $\alpha$ -syn KO mice in the absence of endogenous NCK2, as well as in primary neurons with different overexpression

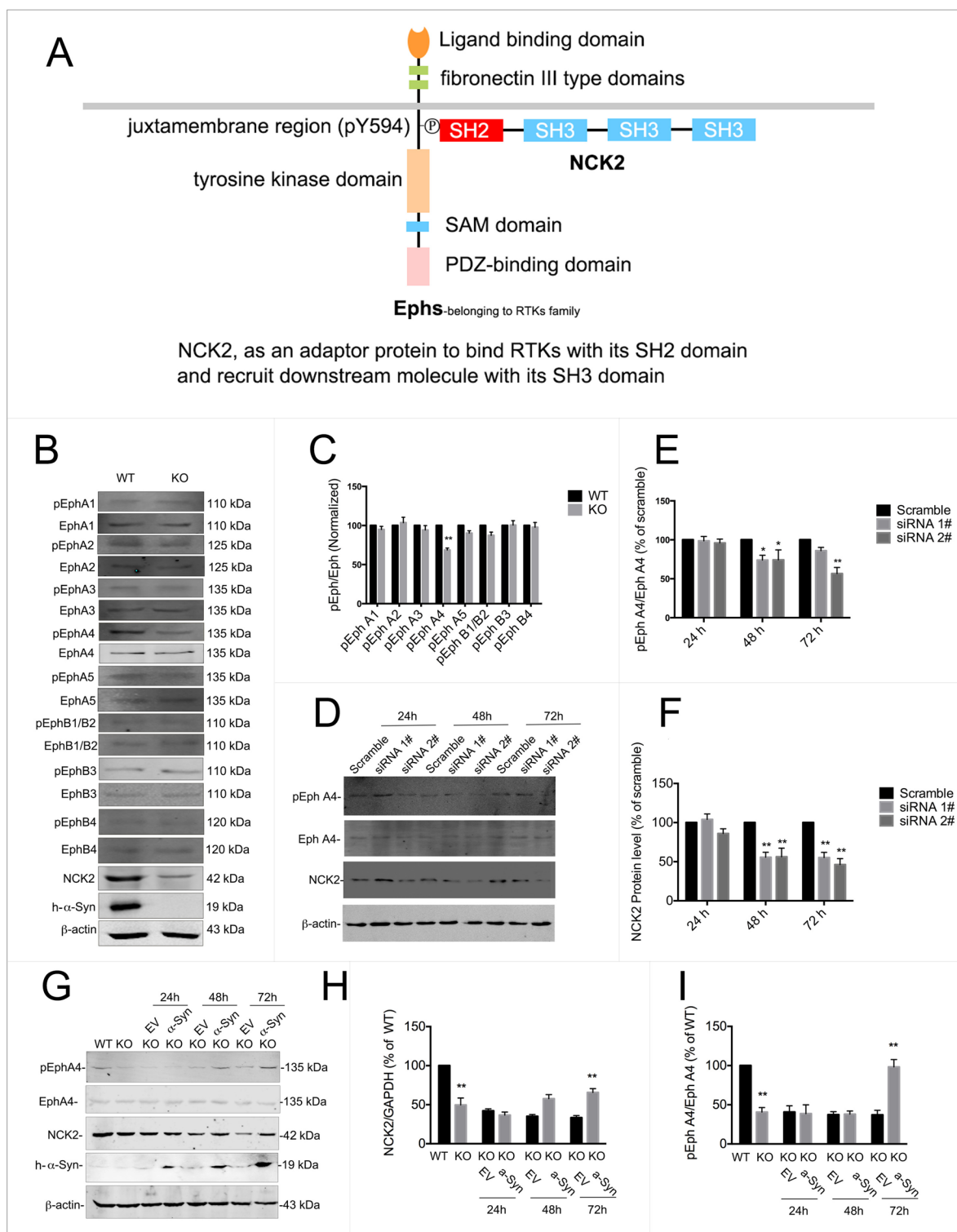


**Fig. 6** EphA4 was inactivated with α-syn or NCK2 deficiency. **A** A model graph for NCK2 binding Ephs. **B, C** All 9 phosphorylated Ephrin receptors were detected by western blot. As shown above, the phosphorylation level of EphA1, EphA2, EphA3, EphA5, EphB1/B2, EphB3 and EphB4 were not changed. However, phosphorylated Eph A4 level was down-regulated with α-syn deficiency. **D, F** Knocking-down of NCK2 also led to down-regulation of phosphorylated Eph A4. **G-I** The primary cultured α-syn<sup>-/-</sup> neurons were transfected with LV-α-syn. NCK2 and phosphorylated EphA4 were down-regulated in α-syn<sup>-/-</sup> neurons. The down-regulation of NCK2 and phosphorylated EphA4 were reversed by overexpression of α-syn. Data are expressed as mean ± SD. \*p < 0.05, \*\*p < 0.01 compared to WT or scramble, respectively; n = 3

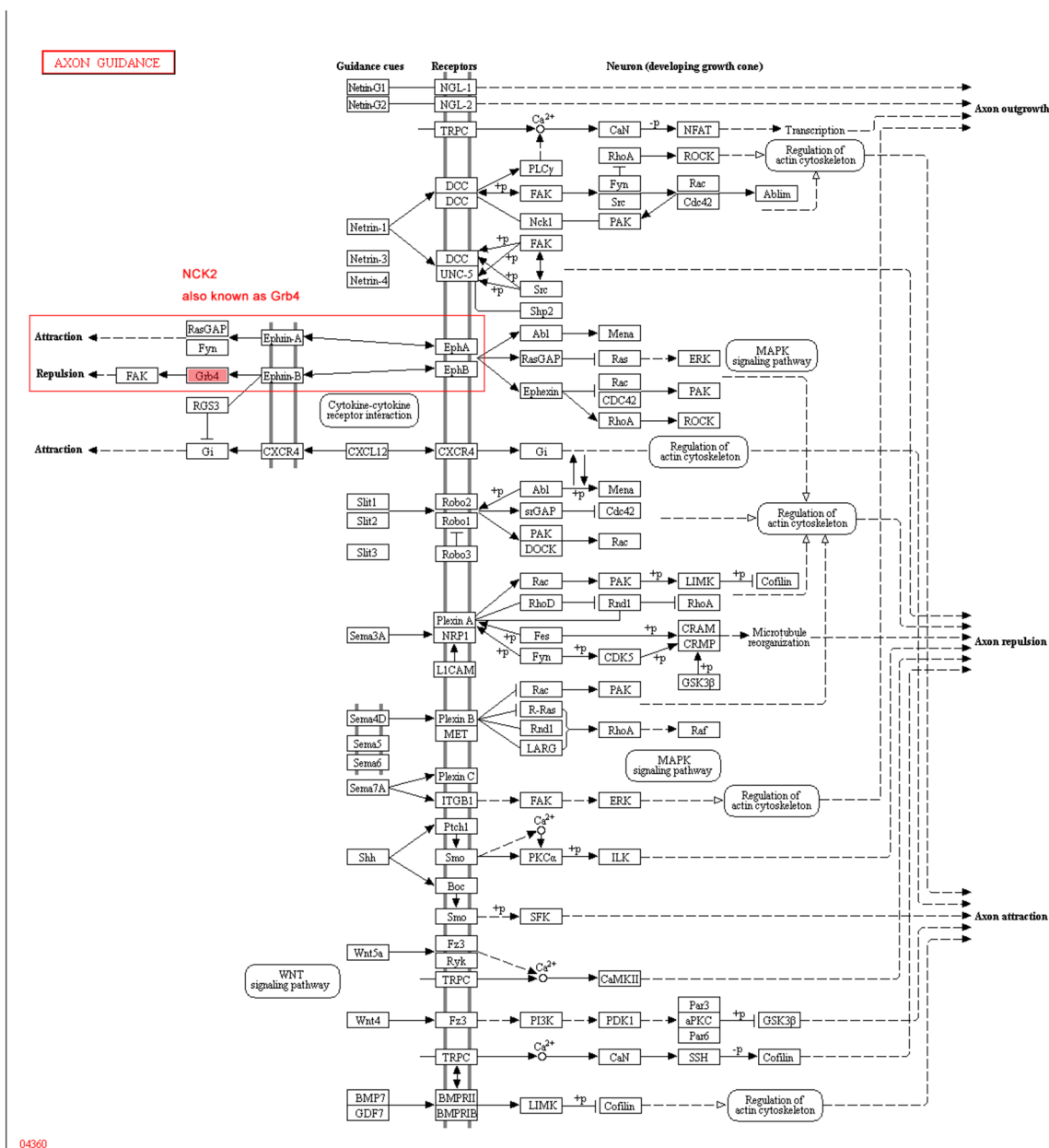


**Fig. 7** Axon guidance pathway analysis. The axon guidance pathway showed that both Ephrin A/Eph A and Ephrin B/EphB receptor signaling pathway involved in axon guidance, either on repulsion or attraction by cooperation with NCK2

levels of  $\alpha$ -syn and NCK2. The level of active RhoA in KO neurons were greatly reduced with lower level of NCK2, increased in neurons overexpressing small dosage of  $\alpha$ -syn and NCK2 and decreased to be lower than WT control in neurons with higher expression of  $\alpha$ -syn and NCK2 (Fig. 9C). These results suggested that NCK2 acted as an upstream regulator of RhoA and that the role toward Rho A activity can be either positive or negative depending on the relative amount of its protein level. This concentration-dependent manner is a typical

biphasic scaffold effect, as similarly shown by studies on BPGAP1 [29].

**Discussion**

It was reported that  $\alpha$ -syn null mice display striking resistance to MPTP-induced degeneration of Dopaminergic neurons and DA release, and this resistance appears to result from an inability of the toxin to inhibit complex I [30]. But later Abeliovich et al. showed that mice lacking  $\alpha$ -syn displayed a reduction in striatal DA and

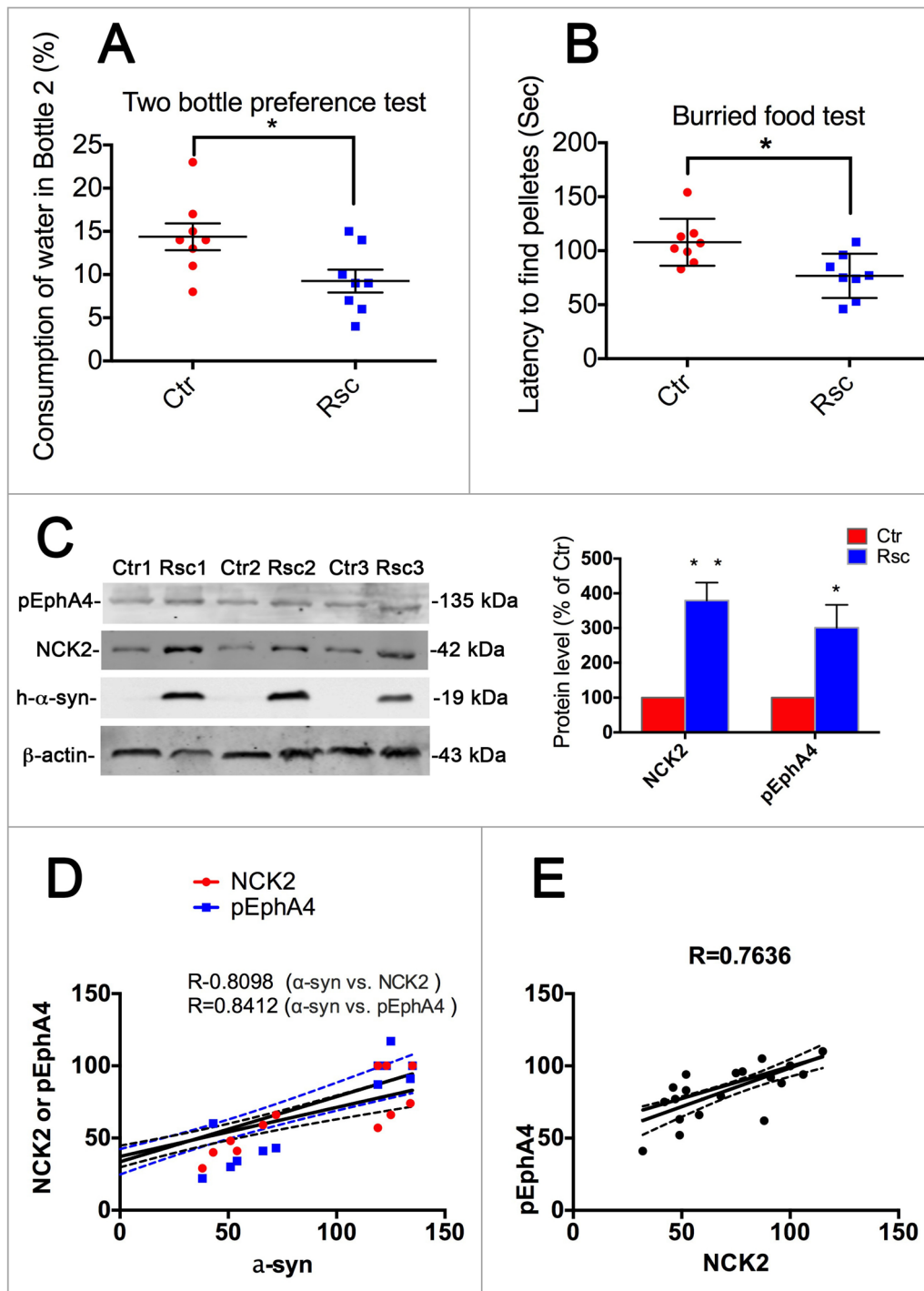


**Fig. 8** Overexpression of  $\alpha$ -syn reversed the down-regulation of NCK2 and pEphA4 and rescued the olfactory dysfunction of  $\alpha$ -syn KO mice accordingly. **A, B** Two bottle preference test and burried food test. Data are expressed as mean  $\pm$  SEM. \* $p < 0.05$ ;  $n = 8$ . **C** Western blot for NCK2 and pEphA4. Data are expressed as mean  $\pm$  SEM. \* $p < 0.05$ ;  $n = 3$ . **D** Correlation analysis among  $\alpha$ -syn, NCK2 and pEphA4.  $R = 0.8098$   $\alpha$ -syn vs. NCK2,  $R = 0.8412$   $\alpha$ -syn vs. pEphA4. **E** Correlation analysis between NCK2 and pEphA4.  $R = 0.7636$

an attenuation of DA-dependent locomotor response to amphetamine [31]. These findings support the hypothesis that  $\alpha$ -syn is an essential protein in central nervous

system. It plays an important role in many physiological functions in vivo. Up to now, the physiological function of  $\alpha$ -syn that was reported include: 1)  $\alpha$ -syn functions in

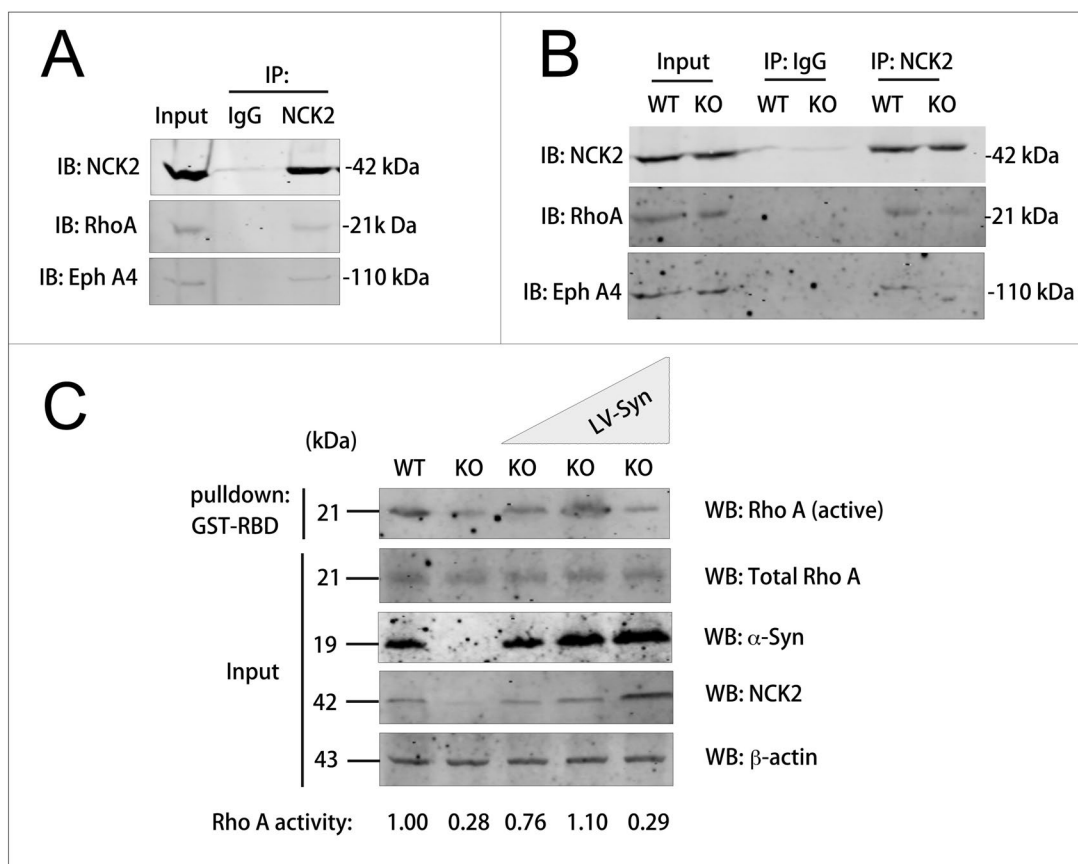


**Fig. 9** NCK2 were associated with EphA4 and Rho A and acted as an upstream regulator of Rho A **A** NCK2 interacted with EphA4 and Rho A under physiological conditions. Tissue lysates of C57BL/6J mice were incubated with NCK2 antibody or immunoglobulin G (IgG) control for immunoprecipitation and then Western blotted with NCK2, EphA4 and Rho A antibodies. Both EphA4 and Rho A were pulled-down with NCK2 antibody. **B** Cell lysates of primary neurons from *Snac*<sup>-/-</sup> mice (KO) or its littermate WT control (WT) were immunoprecipitated with anti-NCK2 antibodies and Western blotted with EphA4 and Rho A antibodies. Less EphA4 and Rho A were pulled-down in  $\alpha$ -syn<sup>-/-</sup> neurons compared with WT control. **C** Endogenous Rho A activity of primary neurons were examined in the presence of different amounts of NCK2. Lysates of  $\alpha$ -syn<sup>-/-</sup> neurons or  $\alpha$ -syn<sup>+/+</sup> neurons or transiently overexpressing gradually increasing amount of  $\alpha$ -syn (illustrated by blue triangle) were used for pull-down with immobilized glutathione S-transferase (GST)-RBD (GST-RBD) of rhotekin and then western blotted with RhoA, NCK2,  $\alpha$ -syn and  $\beta$ -actin antibodies. The ratio of active Rho A to total Rho A is normalized to WT control in lane 1 and labeled at the bottom

synaptic neurotransmitter release by binding to synaptic vesicles and regulating synaptic vesicle pool organization [32, 33]. 2)  $\alpha$ -syn, a presynaptic protein that plays a crucial role in dopamine compartmentalization in the striatum, is also involved in the compartmentalization of norepinephrine in the dentate gyrus [34]. 3)  $\alpha$ -syn modulates brain glucose metabolism because  $\alpha$ -syn deficiency leads to increased glyoxalase I expression and glycation stress [35]. 4) What's more, it was shown that  $\alpha$ -syn/*Snac* KO mice had decreased striatal dopamine and altered dopamine release, uptake in response to electrical stimuli, which suggests that  $\alpha$ -syn may have a role in dopamine neurotransmission [36]. And similarly Connor-Robson et al. reported that stabilization of the striatal DA level depends on the presence of  $\alpha$ -syn and cannot be compensated by other family members [37].  $\alpha$ -syn modulates

dopaminergic neuron development, DA reuptake and stabilizes striatal DA level [36–38]. 5)  $\alpha$ -syn modulates microglial phenotype and neuroinflammation [39, 40]. 6) in Kokhan et al.'s experiment,  $\alpha$ -syn/*Snac* KO mice have cognitive impairments [41].  $\alpha$ -syn/*Snac* KO mice showed impaired spatial learning and working memory. 7) Using co-immunoprecipitation techniques, Alim et al. found  $\alpha$ -syn significantly interacts with tubulin and that  $\alpha$ -syn may behave as a potential microtubule-associated protein [42]. Here we report a novel function of  $\alpha$ -syn that it is essential for OSNs axon projection.  $\alpha$ -syn was highly expressed in both olfactory epithelium and OB. Lacking of  $\alpha$ -syn induced aberrant projection of OSNs.

188 differentially expressed proteins resulted from  $\alpha$ -syn deficiency were identified by iTraQ based LC-MS. 9 of them were associated with axon guidance, including

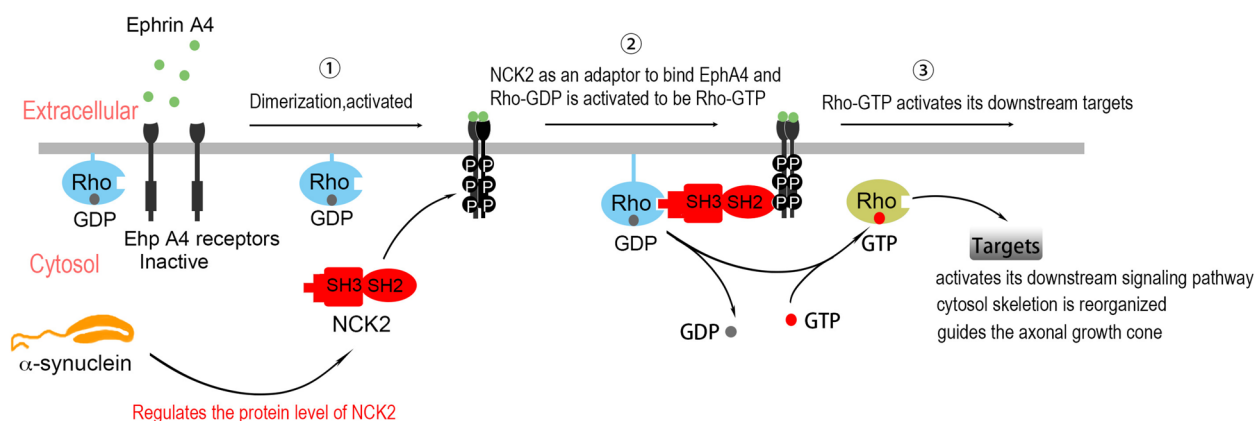


**Fig. 10**  $\alpha$ -syn modulates NCK2-EphA4/RhoA pathway by regulating NCK2 protein level

Cdh4, Cldn5, Dscam, Eif2b2, Pllp, Snapin, Spag1, Stk11, and NCK2. These results suggest that Cdh4, Cldn5, Dscam, Eif2b2, Pllp, Snapin, Spag1, Stk11, NCK2 may be involved in the modulation of olfactory neurons projection by  $\alpha$ -syn. In the present study, we further confirmed that NCK2 was down-regulated in  $\alpha$ -syn<sup>-/-</sup> mice both in mRNA and protein level. NCK2 belongs to a family of adaptor proteins and NCK2 is located in chromosome 2. The protein contains three SH3 domains and one SH2 domain. The protein has no known catalytic function but has been shown to bind and recruit various proteins involved in the regulation of RTKs. It is through these regulatory activities that this protein is believed to be involved in cytoskeletal reorganization. In the present study, we examined NCK2 targeted receptor protein tyrosine kinases Ephrin family and found that EphA4 was deactivated in  $\alpha$ -syn<sup>-/-</sup> mice. Down-regulation of NCK2 and deactivation of Eph4 can be reversed by overexpression of  $\alpha$ -syn, indicating that NCK2-Eph A4 signaling pathway was responsible, at least partially responsible for this  $\alpha$ -syn mediated aberrant projection.

It was reported that NCK2 belongs to the adaptor protein family. It binds to the phosphorylated tyrosine residue of the upstream signal protein via SH2 domain and binds to the proline rich domain of the downstream signal protein via SH3 domain [43]. The junction protein achieves signal transmission between upstream and downstream signaling proteins through this connection. In the present study, we found that NCK2 was associated with Eph A4, and Rho A. Nonetheless, Rho A activity was lower in  $\alpha$ -syn deficient mice, indicating that NCK2 binds Eph A4 and RhoA, further activating Rho A. Rho A, as a mammalian gene homolog of the Ras family, is a member of the Rho subfamily of the small molecular weight GTPase superfamily. Rho is regulated by various cytokines; GTP enzyme activating proteins (GAPs)

and GDP dissociation inhibitors (GDIs) are Rho in-activators. Activators can enable Rho A to release GDP and combine with GTP; GAPs can activate the GTP enzyme activity of Rho A molecules themselves. Hydrolyze GTP into GDP; GDIs can suppress the transition between Rho GDP and Rho GTP states. Under the regulatory action of the above mentioned molecules, Rho completes the transition between the two states to achieve the "molecular switching" effect in its signal transduction process [44]. Activated Rho GTP combines with its downstream targets eg. Rho kinase (ROCK) to activate the latter, causing recombination of Cytoskeleton [45].

In the physiological conditions, Eph A4 receptors were activated by their ligands Ephrin A4. NCK2, as an adaptor, binds to Eph A4 and Rho A-GDP. RhoA-GDP was phosphorylated to be Rho A-GTP (the active form of Rho A). The Rho A-GTP further activated its downstream signaling pathway and cytosol skeleton was reorganized. NCK2 protein level was regulated by  $\alpha$ -syn. Hence, NCK2 protein level is not sufficient in  $\alpha$ -syn/Snac KO mice. That is the molecular mechanism why OSNs projected aberrantly and resulted in mice hyposmia.

There are still some limitation present in the current study. Eg. the mechanism that  $\alpha$ -syn regulates NCK2 protein level is still unclear. But it was reported that  $\alpha$ -syn is abundant in nucleus and it regulate several other genes transcription as a transcriptional factor [46, 47]. Hence, it is possible that  $\alpha$ -syn transcriptionally modulate NCK2 gene expression and protein translation accordingly. However, further experimental research is required to elucidate. In addition, in the process of  $\alpha$ -syn deficiency induced hyposmia, we cannot rule out the possibility that  $\alpha$ -syn also participates in olfactory regulation by influencing other factors except for NCK2. Also, we are using  $\alpha$ -syn whole body KO model which cannot rule out the

interference of changes in other tissues or organs on the sense of smell. These need to be explored through more research in the future.

## Conclusions

Our study suggests that  $\alpha$ -syn regulates NCK2 protein level and controls the precise axon guidance of olfactory neurons via NCK2-EphA4/RhoA pathway. NCK2 modulates EphA4/Rho A signaling pathway by interacting with EphA4 and RhoA as an adaptor (Fig. 10).

## Abbreviations

PD	Parkinson's disease
$\alpha$ -syn	$\alpha$ -Synuclein
NAC	Non-amyloid-b component
SNAC <sup>-/-</sup>	Snac/ $\alpha$ -synuclein knockout
WT	Wild-type
KO	Knockout
OB	Olfactory bulb
SCX	Strong cation exchange chromatography
LC	Liquid chromatography
IDA	Information dependent acquisition
CID	Collision-induced dissociation
Crt	Cortex
Cere	Cerebellum
OE	Olfactory epithelium
Str	Striatum
SN	Substantia nigra
OR	Olfactory receptor
RTK	Receptor tyrosine kinase

## Supplementary Information

The online version contains supplementary material available at <https://doi.org/10.1186/s13578-024-01313-6>.

Supplementary Material 1.

## Acknowledgements

We thank Dr. Yan Zhou and Ms. Xiaohong Sun of Capital Medical University for technique supports.

## Author contributions

J.R. and L.L. conceived and designed the experiments. L.L., F.G. M and N. C. funded and supervised the research. J.R. and C.W. performed experiments. M.X.Z., J.J.Y. and M.Q.Q. performed data analysis. G.G., Y.W.J., T.F. Z and N.X. assisted the experiments. J.R. and L.L. wrote and edited the manuscript.

## Funding

This work was supported by grants from the National Natural Science Foundation of China (81830033, 81971070), Natural Science Foundation of Beijing (7192017), Scientific Research Common Program of Beijing Municipal Commission of Education (KM201710025001).

## Availability of data and materials

The data that support the findings of this study are available from the corresponding author upon reasonable request.

## Declarations

### Ethics approval and consent to participate

Our animal protocol was approved by the Institutional Animal Care and Use Committee of Capital Medical University in accordance with the Basel Declaration (Approval No: AEEI-2020-104; Date: Sep. 2020).

## Consent for publication

Not applicable.

## Competing interests

The authors declare no competing interests.

Received: 7 June 2024 Accepted: 14 October 2024

Published online: 14 November 2024

## References

- Schneider SA, Obeso JA. Clinical and pathological features of Parkinson's disease. *Curr Top Behav Neurosci*. 2015;22:205–20.
- Elsayed I, Martinez-Carrasco A, Cornejo-Olivas M, Bandres-Ciga S. Mapping the diverse and inclusive future of Parkinson's disease genetics and its widespread impact. *Genes*. 2021;12(11):1681–93.
- De Miranda BR, Goldman SM, Miller GW, Greenamyre JT, Dorsey ER. Preventing Parkinson's disease: an environmental agenda. *J Parkinsons Dis*. 2022;12(1):45–68.
- Barba L, Paolini PF, Bellomo G, Gaetani L, Halbgebauer S, Oeckl P, Otto M, Parnetti L. Alpha and beta synucleins: from pathophysiology to clinical application as biomarkers. *Mov Disord*. 2022;37(4):669–83.
- Burré J, Sharma M, Südhof TC. Cell biology and pathophysiology of  $\alpha$ -synuclein. *Cold Spring Harb Perspect Med*. 2018;8(3):a024091.
- Villar-Piqué A, LopesdaFonseca T, Outeiro TF. Structure, function and toxicity of alpha-synuclein: the Bermuda triangle in synucleinopathies. *J Neurochem*. 2016;139(S1):240–55.
- Sulzer D, Edwards RH. The physiological role of  $\alpha$ -synuclein and its relationship to Parkinson's Disease. *J Neurochem*. 2019;150(5):475–86.
- Sarchione A, Marchand A, Taymans JM, Chartier-Harlin MC. Alpha-synuclein and lipids: the elephant in the room? *Cells*. 2021;10(9):2452.
- Zella MAS, Metzendorf J, Ostendorf F, Maass F, Muhlack S, Gold R, Haghikia A, Tönges L. Novel immunotherapeutic approaches to target alpha-synuclein and related neuroinflammation in Parkinson's disease. *Cells*. 2019;8(2):105.
- Lesage S, Anheim M, Letournel F, Bousset L, Honoré A, Rozas N, Pieri L, Madióna K, Dürr A, Melki R, Verny C, Brice A. G51D  $\alpha$ -synuclein mutation causes a novel Parkinsonian–pyramidal syndrome. *Ann Neurol*. 2013;73(4):459–71.
- Pasanen P, Myllykangas L, Siitonen M, Raunio A, Kaakkola S, Lyytinen J, Tienari PJ, Pöyhönen M, Paetau A. A novel  $\alpha$ -synuclein mutation A53E associated with atypical multiple system atrophy and Parkinson's disease-type pathology. *Neurobiol Aging*. 2014;35(9):2180–5.
- Polymeropoulos MH, Lavedan C, Leroy E, Ide SE, Dehejia A, Dutra A, Pike B, Root H, Rubenstein J, Boyer R, Stenroos ES, Chandrasekharappa S, Athanassiadou A, Papapetropoulos T, Johnson WG, Lazzarini AM, Duvoisin RC, Di Iorio G, Golbe LI, Nussbaum RL. Mutation in the  $\alpha$ -synuclein gene identified in families with Parkinson's disease. *Science*. 1997;276(5321):2045–7.
- Zarranz JJ, Alegre J, Gómez-Esteban JC, Lezcano E, Ros R, Ampuero I, Vidal L, Hoenicka J, Rodriguez O, Atarés B, Llorens V, Gomez Tortosa E, del Ser T, Muñoz DG, de Yébenes JG. The new mutation, E46K, of  $\alpha$ -synuclein causes Parkinson and Lewy body dementia. *Ann Neurol*. 2004;55(2):164–73.
- Appel-Cresswell S, Vilarino-Guell C, Encarnacion M, Sherman H, Yu I, Shah B, Weir D, Thompson C, Szu-Tu C, Trinh J, Aasly JO, Rajput A, Rajput AH, Jon Stoessl A, Farrer MJ. Alpha-synuclein p.H50Q, a novel pathogenic mutation for Parkinson's disease. *Mov Disord*. 2013;28(6):811–3.
- Krüger R, Kuhn W, Müller T, Voitalla D, Graeber M, Kösel S, Przuntek H, Epplen JT, Schöls L, Riess O. AlaSOP mutation in the gene encoding  $\alpha$ -synuclein in Parkinson's disease. *Nat Genet*. 1998;18(2):106–8.
- Farrer M, Kachergus J, Forno L, Lincoln S, Wang DS, Hulihan M, Maraganore D, Gwinn-Hardy K, Wszolek Z, Dickson D, Langston JW. Comparison of kindreds with parkinsonism and  $\alpha$ -synuclein genomic multiplications. *Ann Neurol*. 2004;55(2):174–9.
- Singleton A, Gwinn-Hardy K, Sharabi Y, Li S, Holmes C, Dendi R, Hardy J, Singleton A, Crawley A, Goldstein DS. Association between cardiac denervation and Parkinsonism caused by  $\alpha$ -synuclein gene triplication. *Brain*. 2004;127(4):768–72.

18. Blauwendraat C, Heilbron K, Vallerga CL, Bandres-Ciga S, von Coelln R, Pihlström L, Simón-Sánchez J, Schulte C, Sharma M, Krohn L, Siitonen A, Iwaki H, Leonard H, Noyce AJ, Tan M, Gibbs JR, Hernandez DG, Scholz SW, Jankovic J, Shulman LM, Lesage S, Corvol JC, Brice A, van Hilten JJ, Marinus J, 23andMe Research Team, Eerola-Rautio J, Tienari P, Majamaa K, Toft M, Grosset DG, Gasser T, Heutink P, Shulman JM, Wood N, Hardy J, Morris HR, Hinds DA, Gratten J, Visscher PM, Gan-Or Z, Nalls MA, Singleton AB. Parkinson's disease age at onset genome-wide association study: defining heritability, genetic loci, and  $\alpha$ -synuclein mechanisms. *Mov Disord*. 2019;34(6):866–75.
19. Gámez-Valero A, Beyer K. Alternative splicing of alpha- and beta-synuclein genes plays differential roles in synucleinopathies. *Genes*. 2018;9(2):63.
20. Morato Torres CA, Wassouf Z, Zafar F, Sastre D, Outeiro TF, Schüle B. The role of alpha-synuclein and other Parkinson's genes in neurodevelopmental and neurodegenerative disorders. *Int J Mol Sci*. 2020;21(16):5724.
21. Srinivasan E, Chandrasekar G, Chandrasekar P, Anbarasu K, Vickram AS, Karunakaran R, Rajasekaran R, Srikanth PS. Alpha-synuclein aggregation in Parkinson's disease. *Front Med*. 2021;8: 736978.
22. Tolosa E, Garrido A, Scholz SW, Poewe W. Challenges in the diagnosis of Parkinson's disease. *Lancet Neurol*. 2021;20(5):385–97.
23. Goedert M, Spillantini MG, Del Tredici K, Braak H. 100 years of Lewy pathology. *Nat Rev Neurol*. 2013;9(1):13–24.
24. Obeso JA, Stamelou M, Goetz CG, Poewe W, Lang AE, Weintraub D, Burn D, Halliday GM, Bezard E, Przedborski S, Lehericy S, Brooks DJ, Rothwell JC, Hallett M, DeLong MR, Marras C, Tanner CM, Ross GW, Langston JW, Klein C, Bonifati V, Jankovic J, Lozano AM, Deuschl G, Bergman H, Tolosa E, Rodriguez-Violante M, Fahn S, Postuma RB, Berg D, Marek K, Standaert DG, Surmeier DJ, Olanow CV, Kordower JH, Calabresi P, Schapira AHV, Stoessl AJ. Past, present, and future of Parkinson's disease: a special essay on the 200th Anniversary of the Shaking Palsy. *Mov Disord*. 2017;32(9):1264–310.
25. Lo C, Arora S, Ben-Shlomo Y, Barber TR, Lawton M, Klein JC, Kanavou S, Janzen A, Sittig E, Oertel WH, Grosset DG, Hu MT. Olfactory testing in Parkinson disease and REM behavior disorder: a machine learning approach. *Neurology*. 2021;96(15):e2016–27.
26. Pont-Sunyer C, Hotter A, Gaig C, Seppi K, Compta Y, Katzenschlager R, Mas N, Hofeneder D, Brücke T, Bayés A, Wenzel K, Infante J, Zach H, Pirker W, Posada IJ, Álvarez R, Ispierto L, De Fàbregues O, Callén A, Palasí A, Aguilar M, Martí MJ, Valldeoriola F, Salameo M, Poewe W, Tolosa E. The onset of nonmotor symptoms in Parkinson's disease (The ONSET PD Study). *Mov Disord*. 2015;30(2):229–37.
27. Hawkes CH, Del Tredici K, Braak H. Parkinson's disease. *Ann N Y Acad Sci*. 2009;1170(1):615–22.
28. Hawkes CH, Del Tredici K, Braak H. Parkinson's disease: a dual-hit hypothesis. *Neuropathol Appl Neurobiol*. 2007;33(6):599–614.
29. Jiang T, Pan CQ, Low BC. BPGAP1 spatially integrates JNK/ERK signaling crosstalk in oncogenesis. *Oncogene*. 2017;36(22):3178–92.
30. Dauer W, Kholodilov N, Vila M, Trillat AC, Goodchild R, Larsen KE, Staal R, Tieu K, Schmitz Y, Yuan CA, Rocha M, Jackson-Lewis V, Hersch S, Sulzer D, Przedborski S, Burke R, Hen R. Resistance of alpha-synuclein null mice to the Parkinsonian neurotoxin MPTP. *Proc Natl Acad Sci U S A*. 2002;99(22):14524–9.
31. Abeliovich A, Schmitz Y, Fariñas I, Choi-Lundberg D, Ho WH, Castillo PE, Shinsky N, Verdugo JM, Armanini M, Ryan A, Hynes M, Phillips H, Sulzer D, Rosenthal A. Mice lacking alpha-synuclein display functional deficits in the nigrostriatal dopamine system. *Neuron*. 2000;25(1):239–52.
32. Carnazza KE, Komer LE, Xie YX, Pineda A, Briano JA, Gao V, Na Y, Ramlall T, Buchman VL, Eliezer D, Sharma M, Burré J. Synaptic vesicle binding of  $\alpha$ -synuclein is modulated by  $\beta$ - and  $\gamma$ -synucleins. *Cell Rep*. 2022;39(2): 110675.
33. Vargas KJ, Schrod N, Davis T, Fernandez-Busnadiego R, Taguchi YV, Laugks U, Lucic V, Chandra SS. Synucleins have multiple effects on presynaptic architecture. *Cell Rep*. 2017;18(1):161–73.
34. Yavich L, Jäkälä P, Tanila H. Abnormal compartmentalization of norepinephrine in mouse dentate gyrus in  $\alpha$ -synuclein knockout and A30P transgenic mice. *J Neurochem*. 2006;99(3):724–32.
35. Kurz A, Rabbani N, Walter M, Bonin M, Thornalley P, Auberger G, Gisbert S. Alpha-synuclein deficiency leads to increased glyoxalase I expression and glycation stress. *Cell Mol Life Sci*. 2011;68(4):721–33.
36. Chadchankar H, Ihalainen J, Tanila H, Yavich L. Decreased reuptake of dopamine in the dorsal striatum in the absence of alpha-synuclein. *Brain Res*. 2011;1382:37–44.
37. Connor-Robson N, Peters OM, Millership S, Ninkina N, Buchman VL. Combinational losses of synucleins reveal their differential requirements for compensating age-dependent alterations in motor behavior and dopamine metabolism. *Neurobiol Aging*. 2016;46:107–12.
38. Tarasova TV, Lytkina OA, Roman AY, Bachurin SO, Ustyugov AA. The role of alpha-synuclein in the development of the dopaminergic neurons in the substantia nigra and ventral tegmental area. *Doklady Biol Sci*. 2016;466(1):5–7.
39. Austin SA, Rojanathammanee L, Golovko MY, Murphy EJ, Combs CK. Lack of alpha-synuclein modulates microglial phenotype in vitro. *Neurochem Res*. 2012;36(6):994–1004.
40. Ertle B, Kuhbandner K, Jörg S, Hoffmann A, Winkler J, Linker RA.  $\alpha$ -Synuclein deficiency promotes neuroinflammation by increasing Th1 cell-mediated immune responses. *J Neuroinflamm*. 2016;13(1):201.
41. Kokhan VS, Afanasyeva MA, Van'kin GI.  $\alpha$ -Synuclein knockout mice have cognitive impairments. *Behav Brain Res*. 2012;231(1):226–30.
42. Alim MA, Ma QL, Takeda K, Aizawa T, Matsubara M, Nakamura M, Asada A, Saito T, Kaji H, Yoshii M, Hisanaga S, Ueda K. Demonstration of a role for  $\alpha$ -synuclein as a functional microtubule-associated protein. *J Alzheimer's Dis*. 2004;6:435–42.
43. Alfaidi M, Scott ML, Orr AW. Sinner or Saint?: Nck adaptor proteins in vascular biology. *Front Cell Dev Biol*. 2021;9: 688388.
44. Schmidt SI, Blaabjerg M, Freude K, Meyer M. RhoA signaling in neurodegenerative diseases. *Cells*. 2022;11(9):1520.
45. Lin Y, Watanabe-Chailland M, Zheng Y. Protocol for structural and biochemical analyses of RhoA GTPase. *STAR Protoc*. 2021;2(2): 100541.
46. Li YH, Gao N, Ye YW, Li X, Yu S, Yang H, Ueda K, Chan P. Alpha-synuclein functions as a negative regulator for expression of tyrosine hydroxylase. *Acta Neurol Belg*. 2011;111:130–5.
47. Davidi D, Schechter M, Elhadi SA, Matatov A, Nathanson L, Sharon R. Synuclein translocates to the nucleus to activate retinoic-acid-dependent gene transcription. *iScience*. 2020;23(3): 100910.

## Publisher's Note

Springer Nature remains neutral with regard to jurisdictional claims in published maps and institutional affiliations.